Evolution of the N=50 shell gap energy towards ^{78}Ni

J. Hakala, S. Rahaman, V.-V. Elomaa, T. Eronen, U. Hager,* A. Jokinen, A. Kankainen, I. D. Moore, H. Penttilä, S. Rinta-Antila,† J. Rissanen, A. Saastamoinen, T. Sonoda,‡ C. Weber, and J. Äystö§
Department of Physics, P.O. Box 35 (YFL), FI-40014 University of Jyväskylä, Finland
(Dated: June 27, 2008)

Atomic masses of the neutron-rich isotopes $^{76-80}$Zn, $^{78-83}$Ga, $^{80-85}$Ge, $^{81-87}$As and $^{84-89}$Se have been measured with high precision using the Penning trap mass spectrometer JYFLTRAP at the IGISOL facility. The masses of ^{82,83}Ga, $^{83-85}$Ge, $^{84-87}$As and ^{89}Se were measured for the first time. These new data represent a major improvement in the knowledge of the masses in this neutron-rich region. Two-neutron separation energies provide evidence for the reduction of the N=50 shell gap energy towards germanium (Z=32) and a subsequent increase at gallium (Z=31). The data are compared with a number of theoretical models. An indication of the persistent rigidity of the shell gap towards nickel (Z=28) is obtained.

PACS numbers: 21.10.Dr, 21.60.-n, 27.50.+e

arXiv:0806.4489v1 [nucl-ex] 27 Jun 2008

Evolution of the shell structure of nuclei with extreme neutron-richness is an increasingly important field of study in nuclear structure physics and nuclear astrophysics. A specific issue of major interest in recent years has been the question of whether the magic nucleon numbers as known in the valley of stability survive at large values of isospin [1, 2] and the possible role of the mutual support of magicities observed in or near the valley of stability in the case of exotic nuclei [3]. In this context, several experimental studies on excited states have been performed to probe the evolution of the $N = 50$ neutron shell far from stability. They have provided data on energies of the lowest excited states of even-Z $N = 49$ and $N = 51$ nuclei, particle-hole excitations of even-even nuclei across the N=50 shell as well as B(E2) values for the ground state transitions of ^{78,80,82}Ge and ^{74,76,78,80}Zn. The experimental techniques employed include beta-delayed gamma-ray spectroscopy of neutron-rich Cu, Zn and Ga [4, 5, 6, 7], isomeric gamma-ray spectroscopy of ^{76}Ni [8], deep-inelastic studies of N=50 nuclei ^{87}Rb, ^{85}Br, ^{84}Se and ^{82}Ge [9] and of excited fission fragments of ^{82}Ge, ^{84}Se, ^{84,85}Br[10, 11, 12]. Very recently experiments employing post-accelerated radioactive ion beams of ^{78,80,82}Ge [13, 14] and ^{74,76,78,80}Zn [15] have also been successfully performed.

All current experimental results and particularly their interpretation in the framework of the shell model indicate a weakening of the $N = 50$ shell gap towards Ge ($Z = 32$). Furthermore there is evidence that the gap increases in the region of Zn [15]. The interpretation, however, is very sensitive to the effective interaction and core polarisation effects. Accordingly the quantitative verification of the evolution of the shell gap energy has been missing so far. Prior to the present work the experimental knowledge [16] of two-neutron separation energies (S_{2n}) across N=50 indicated the reduction of the shell gap, i.e. the difference of S_{2n} values between the N=50 and N=52 isotones, from Z=40 down to Z=34. However, no conclusive trend for the evolution of this gap further from stability can be determined without new experimental results. The previous mass data [16] in this region are often associated with large systematic errors as observed in our previous studies [17, 18]. In this Letter we present new data from high-precision mass measurements of neutron-rich Zn, Ga, Ge, As and Se isotopes obtained by employing a Penning trap technique [19].

The measurements were performed using the JYFLTRAP Penning trap setup [20] which is connected to the Ion Guide Isotope Separator On-Line (IGISOL) facility. The ions of interest were produced in proton-induced fission reactions by bombarding a 15 mg/cm^2 thick natural uranium target with a proton or deuteron beam of 25 MeV energy. The fission reaction products were stopped in a helium-filled gas cell at a pressure of about 200 mbar, and due to charge-exchange processes with the gas, the ions ended up mostly singly charged. The helium flow then transported the ions out of the gas cell towards the sextupole ion guide (SPIG). After extraction the ions were accelerated to 30 keV and separated by a 55° bending magnet so that ions with the selected mass number were guided into a gas-filled radio frequency quadrupole (RFQ) cooler and buncher. The RFQ cooler was used to cool and store the ions before releasing them in a short bunch towards the Penning trap setup.

In a Penning trap ions have three different eigenmotions: independent axial motion and two coupled radial motions, magnetron (ν_-) and reduced cyclotron (ν_+). The frequencies of the radial motions sum to a true cyclotron frequency $\nu_c = \nu_- + \nu_+$. The JYFLTRAP setup consists of two cylindrical Penning traps, the purification and precision trap, which are located inside a 7 T superconducting magnet. In the purification trap filled with helium buffer gas, the ions were further cooled by mass selective cooling and cleaned from isobaric contaminants. After being transported to the precision trap through a narrow diaphragm, the magnetron radius of the ions was increased by a dipole excitation. A quadrupole ex-

citation was subsequently applied so that the magnetron motion of the ions was converted to cyclotron motion, whereby the ions gained radial energy. This energy gain was largest for the resonance frequency $\nu_c = \frac{qB}{2\pi m}$ of the ion cyclotron motion. Here q and m are the charge and mass of the ions, and B is the magnetic field. Finally, the ions were ejected towards a microchannel plate (MCP) detector for measuring their time-of-flight (TOF). A typical TOF resonance and the corresponding fit are shown in Fig. 1 where the fit is based on equations presented in [21]. The experimental setup and measurement technique are described in more detail in [17, 18].

Using the cyclotron frequencies of an unknown species (m_{meas}) and a well-known reference ion (m_{ref}) and the mass of the electron (m_e), a precise mass determination for singly charged ions can be made:

$$m_{meas} = \frac{\nu_{c,ref}}{\nu_{c,meas}} (m_{ref} - m_e) + m_e. \qquad (1)$$

The masses of $^{76-80}$Zn, $^{78-83}$Ga, $^{80-85}$Ge, $^{81-87}$As and $^{84-89}$Se were measured during six different beam times (see Table I). Excitation times between 200 ms and 900 ms were used depending on the half-life of each isotope. An excitation pattern with time-separated oscillatory fields (Ramsey excitation) [22] was used in the measurements in October 2007. Each isotope was measured typically three to five times and before and after each measurement a similar measurement was performed for the reference isotope ^{88}Rb that has a mass excess of -82609.00 ± 0.16 keV.

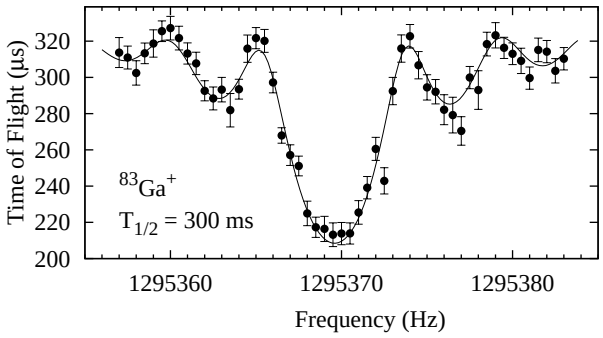

FIG. 1: A typical time-of-flight (TOF) resonance from the JYFLTRAP setup for $^{83}Ga^+$.

The obtained average frequency ratios $\bar{r} = \frac{\nu_{c,ref}}{\nu_{c,meas}}$ and the corresponding mass-excess values are given in Table I. The systematic uncertainties due to the presence of contaminating ions in the trap, the magnetic field fluctuations and the mass difference $A_{meas} - A_{ref}$ between the reference ion and the ion of interest were taken into account in the cyclotron frequency ratio determination. In order to reduce the effect due to ion-ion interactions in the trap the count-rate was kept low by controlling the beam gate before the RFQ cooler [17, 18]. This effect was taken into account by applying the count rate class analysis method described in [23] when analysing the data. In the case of low statistics this analysis was not possible and an estimate for the uncertainty was determined based on the analysis made for the closest neighbouring isotope possible. The linear drift of the magnetic field was taken into account by the interpolation of the reference cyclotron frequencies measured before and after the ion of interest. The magnetic field fluctuation beyond the linear drift was experimentally determined to be $3.2(2) \times 10^{-11}$/min [24] before the magnet quenched in June 2007 and $5.7(8) \times 10^{-11}$/min after re-energising the magnet. This value, multiplied by the time difference between two consecutive reference measurements, was added quadratically to each frequency ratio uncertainty. A mass-dependent systematic uncertainty of 7×10^{-10}/u was added quadratically to the final frequency ratio uncertainty. For a consistency check we have compared our measurements of ^{78}Ga and ^{81}As with previous high-precision [25, 26] measurements. In addition we have measured ^{79}Ga in two different beamtimes and our values, -62547.8(22) keV and -62547.5(29) keV, are in excellent agreement with each other. In the case of ^{82}As both the isomer and the ground state were observed with their mass difference in good agreegment with [27].

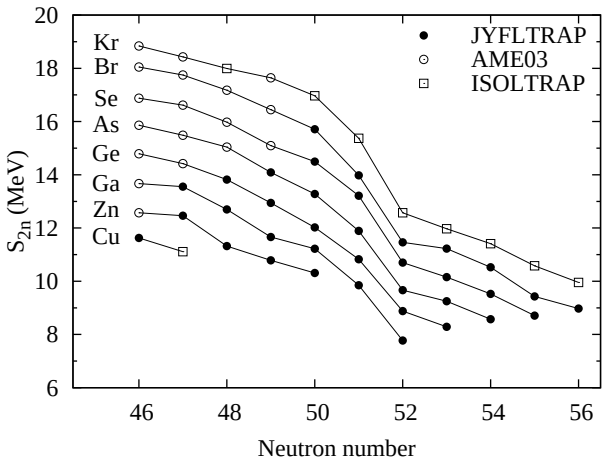

FIG. 2: Two-neutron separation energies for elements with proton number between $Z = 29$ and $Z = 36$.

Figure 2 displays the first-order derivative of the masses, the S_{2n} values of neutron-rich $Z = 29$–36 isotopes calculated from the mass-excess values measured by JYFLTRAP (Table I and [18, 24]) and ISOLTRAP [28]. The new data from JYFLTRAP are shown as filled circles. The occurrence of the closed neutron shell at $N = 50$ is clearly visible from Kr ($Z = 36$) all the way down to Ga ($Z = 31$), manifesting itself in a steep decrease of the S_{2n} values for all nuclei with $N = 51$ and $N = 52$.

In order to gain a more quantitative insight into the evolution of the change of masses around shell closures, one can study the two-nucleon gaps [1, 29] for neutrons or

TABLE I: Obtained cyclotron frequency ratios and resulting mass-excess values in keV from this work. AME03 values based on extrapolation are marked with #. The index a denotes the use of two-fringe Ramsey excitation.

Isotope	$\bar{r} = \frac{\nu_{c,ref}}{\nu_{c,meas}}$	JYFLTRAP	AME03
^{76}Zn	0.863745911(28)	-62303.8(23)^a	-62140(80)
^{77}Zn	0.875163997(51)	-58789.5(42)	-58720(120)
^{78}Zn	0.886555123(33)	-57483.0(27)^a	-57340(90)
^{79}Zn	0.897979777(33)	-53430.9(27)^a	-53420(260$^\#$)
^{80}Zn	0.909376692(83)	-51650(7)	-51840(170)
^{78}Ga	0.886479142(37)	-63704.9(30)^a	-63706.6(24)
^{79}Ga	0.897868446(23)	-62547.6(19)^a	-62510(100)
^{80}Ga	0.909284208(35)	-59223.7(29)	-59140(120)
^{81}Ga	0.920678866(40)	-57628.0(33)	-57980(190)
^{82}Ga	0.932111398(29)	-52930.8(24)	-53100(300$^\#$)
^{83}Ga	0.943531430(32)	-49257.2(26)	-49390(300$^\#$)
^{80}Ge	0.909158285(25)	-69535.3(21)	-69515(28)
^{81}Ge	0.920573067(25)	-66291.7(21)	-66300(120)
^{82}Ge	0.931958942(27)	-65415.1(22)	-65620(240)
^{83}Ge	0.943388317(30)	-60976.5(25)	-60900(200$^\#$)
^{84}Ge	0.954798023(39)	-58148.4(32)	-58250(300$^\#$)
^{85}Ge	0.966234558(45)	-53123.4(37)	-53070(400$^\#$)
^{81}As	0.920496845(37)	-72533.3(30)	-72533(6)
^{82}As	0.931901693(52)	-70103.1(43)	-70320(200)
^{82m}As	0.931903256(46)	-69975.1(38)	-70075(25)
^{83}As	0.943282162(34)	-69669.3(28)	-69880(220)
^{84}As	0.954703930(39)	-65853.5(32)	-66080(300$^\#$)
^{85}As	0.966111638(38)	-63189.1(31)	-63320(200$^\#$)
^{86}As	0.977538428(42)	-58962.1(34)	-59150(300$^\#$)
^{87}As	0.988954438(36)	-55617.9(30)	-55980(300$^\#$)
^{84}Se	0.954580662(24)	-75947.7(20)	-75952(15)
^{85}Se	0.965998990(32)	-72413.5(26)	-72428(30)
^{86}Se	0.977397491(31)	-70503.2(25)	-70541(16)
^{87}Se	0.988822450(27)	-66426.1(22)	-66580(40)
^{88}Se	1.000228663(41)	-63884.1(33)	-63880(50)
^{89}Se	1.011663571(46)	-58992.4(38)	-59200(300$^\#$)

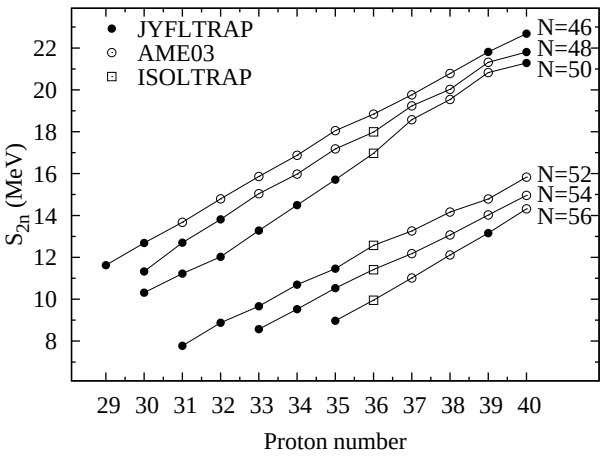

FIG. 3: Two-neutron separation energies for the region of interest plotted as a function of proton number. The evolution of the $N=50$ shell gap is clearly visible.

protons. For magic nuclei the two-nucleon gap energy is approximated by twice the gap in the single-particle spectrum providing a signature for the magicity [29]. For this purpose, we have plotted in Fig. 3 S_{2n} values for even $N=46$–56 isotones as a function of the proton number. The energy difference between the $N=50$ and 52 isotones, corresponding to a two-neutron gap across $N=50$, reveals a trend for the lowering of the shell gap energy towards Ge ($Z=32$). This also corresponds to a minimum in the systematics of the first 2^+ energies of known even-A $N=50$ isotones [9, 10, 11, 12, 13, 14, 15], suggesting a maximal influence of core polarisation effects at this proton number. Fig. 3 also indicates that the gap at $N=50$ opens up when moving further towards Ni ($Z=28$) implying its magic character.

Beyond the energy difference of $N=50$ and 52 isotones, it is of interest to notice that the otherwise smooth trend of S_{2n} values for each isotone is broken between the $N=48$ and 50 isotones. Additional weakening of the two-neutron binding of the $N=50$ isotones between $Z=32$ and 36 might arise, for example, from two-particle two-hole excitations across the shell gap. On the contrary, when comparing the energy differences of the $N=46$, 48 and 52 isotones we observe a rather flat behaviour indicating a smoothness in energies of the $\nu g_{9/2}$ and $\nu d_{5/2}$ (or $\nu s_{1/2}$) neutron states across the entire range of the studied proton numbers.

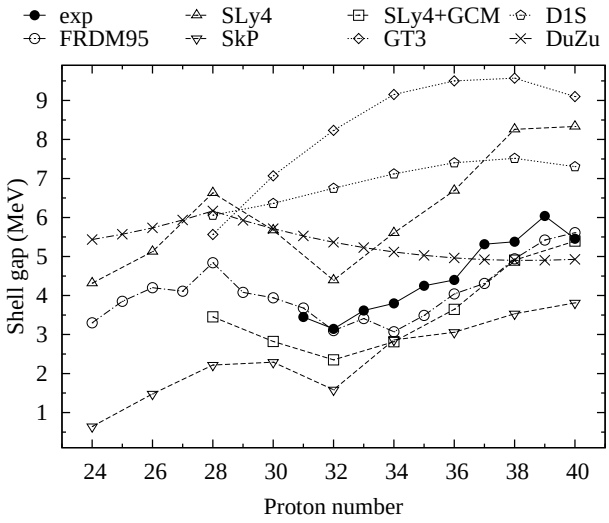

FIG. 4: Evolution of the $N=50$ shell gap and comparison to theoretical models.

The experimental two-neutron shell gap energies $\Delta = S_{2n}(N=50) - S_{2n}(N=52)$ are compared with selected theoretical models in Fig. 4. The models chosen are the Finite Range Liquid-Drop Model (FRDM) which is a well-known sophisticated microscopic-macroscopic model [30], the empirical model of Duflo and Zucker (DuZu) [31], two spherical mean-field calculations by Otsuka *et al.* [2, 32] employing a GT3 tensor or a D1S inter-

action as well as three different self-consistent mean field calculations in the framework of the density functional theory [29, 33, 34]. Both mean-field calculations of Otsuka overpredict the gap by at least a factor of two compared with the experimentally known range. The use of the tensor-based interaction brings the gap clearly down to ^{78}Ni. The best agreement with the data is obtained by the FRDM calculation. Finally, it is remarkable that the models based on the density functional theory reproduce qualitatively the trend observed in this experiment, a monotonic reduction from $Z = 40$ and a minimum at $Z = 32$. They also predict the increase in the gap energy and therefore the strengthening of the magicity towards ^{78}Ni in compliance with the concept of mutual support of magicities [3].

A closer look at Fig. 4 reveals that the calculations of Stoitsov *et al.* with SLy4 and SkP energy density functionals [33, 34] agree in trend but differ in magnitude rather strongly. This could, at least partly, be due to differences in isoscalar effective mass in these two interactions which in turn scales the single-particle level density in the vicinity of the Fermi surface energy with the effective result of a larger gap with SLy4 and a nearly vanishing gap for SkP at $Z = 32$. On the other hand, the similar calculation of Bender *et al.* [29] employing the SLy4 interaction in the deformed basis and adding dynamical quadrupole correlations brings the calculated values closer to those observed in this experiment.

In summary, we have measured the masses of approximately 30 neutron-rich nuclei with unprecedented accuracy to probe experimentally the magicity of the $N = 50$ neutron number far from stability. The data indicates the persistence of this gap towards Ni ($Z = 28$) with an observed minimum at $Z = 32$. This observation is in line with the interpretation of recent spectroscopic data on low-lying excited states of these nuclides in the framework of a shell model. Concerning the binding energies, it is observed that the energy density functional approach can reproduce qualitatively the observed trends in two-neutron separation energies and shell gaps. These high-precision experimental data provide a basis for improved theoretical description of various separation energies of neutron-rich nuclei needed, for example, in nuclear astrophysics. Moreover, the future experiments will have to be pushed towards more exotic nuclei such as ^{82}Zn and ^{81}Cu in the vicinity of ^{78}Ni.

The authors wish to thank Professor Jacek Dobaczewski for inspiring discussions.

This work has been supported by the Academy of Finland under the Finnish Centre of Excellence Programme 2000–2005 (Nuclear and Condensed Matter Physics Programme at JYFL) and the Finnish Centre of Excellence Programme 2006–2011 (Nuclear and Accelerator Based Physics Programme at JYFL).

* Present address: TRIUMF, 4004 Wesbrook Mall, Vancouver, British Columbia, V6T 2A3, Canada
† Present address: Department of Physics, Oliver Lodge Laboratory, University of Liverpool, Liverpool L69 7ZE, UK
‡ Present address: Instituut voor Kern- en Stralingsfysica, Celestijnenlaan 200D, B-3001 Leuven, Belgium
§ Electronic address: juha.aysto@phys.jyu.fi

[1] J. Dobaczewski and W. Nazarewicz, Phil. Trans. R. Soc. London A **356**, 2007 (1998).
[2] T. Otsuka, T. Matsuo, and D. Abe, Phys. Rev. Lett. **97**, 162501 (2006).
[3] N. Zeldes, T. Dumitrescu, and H. Köhler, Nucl. Phys. A **399**, 11 (1983).
[4] O. Perru et al., Eur. Phys. J. A **28**, 307 (2006).
[5] P. Hoff and B. Fogelberg, Nucl. Phys. A **368**, 210 (1981).
[6] J. A. Winger et al. (to be published).
[7] D. Verney et al., Phys. Rev. C **76**, 054312 (2007).
[8] C. Mazzocchi et al., Phys. Lett. B **622**, 45 (2005).
[9] Y. H. Zhang et al., Phys. Rev. C **70**, 024301 (2004).
[10] T. Rzaca-Urban et al., Phys. Rev. C **76**, 027302 (2007).
[11] A. Prévost et al., Eur. Phys. J. A **22**, 391 (2004).
[12] A. Astier et al., Eur. Phys. J. A **30**, 541 (2006).
[13] J. S. Thomas et al., Phys. Rev. C **71**, 021302(R) (2005).
[14] E. Padilla-Rodal et al., Phys. Rev. Lett. **94**, 122501 (2005).
[15] J. V. de Walle et al., Phys. Rev. Lett. **99**, 142501 (2007).
[16] G. Audi, A. Wapstra, and C. Thibault, Nucl. Phys. A **729**, 337 (2002).
[17] U. Hager et al., Phys. Rev. C **75**, 064302 (2007).
[18] S. Rahaman et al., Eur. Phys. J. A **32**, 87 (2007).
[19] K. Blaum, Phys. Rep. **425**, 1 (2006).
[20] A. Jokinen et al., Int. J. Mass Spectr. **251**, 204 (2006).
[21] M. König et al., Int. J. Mass Spectr. **142**, 95 (1995).
[22] S. George et al., Int. J. Mass Spectr. **264**, 110 (2007).
[23] A. Kellerbauer et al., Eur. Phys. J. D **22**, 53 (2003).
[24] S. Rahaman et al., Eur. Phys. J. A **34**, 5 (2007).
[25] C. Guénaut et al., Phys. Rev. C **75**, 044303 (2007).
[26] S. Mordechai et al., Phys. Rev. C **25**, 1276 (1982).
[27] H. Gausemel et al., Phys. Rev. C **70**, 037301 (2004).
[28] P. Delahaye et al., Phys. Rev. C **74**, 034331 (2006).
[29] M. Bender et al., Phys. Rev. C **73**, 034322 (2006).
[30] P. Möller et al., At. Data Nucl. Data Tables **59**, 185 (1995).
[31] J. Duflo and A. P. Zuker, Phys. Rev. C **66**, 051304(R) (2002).
[32] T. Otsuka, private communications (2007).
[33] M. Stoitsov et al., Int. J. Mass Spectr. **251**, 243 (2006).
[34] M. Stoitsov et al., Phys. Rev. C **68**, 054312 (2003).